A Partitioned Fluid-Structure Interaction Approach during Steel Solidification: Application to the Simulation of Ingot Casting

Okba Boughanmi, Michel Bellet

A Partitioned Fluid-Structure Interaction Approach during Steel Solidification: Application to the simulation of Ingot Casting

O. Boughanmi*[1], M. Bellet*[2]

**MINES ParisTech, Centre de Mise en Forme des Matériaux (CEMEF), UMR CNRS 7635, Sophia Antipolis, France*

Keywords: solidification, thermo-mechanical problem, fluid-structure interaction, two-step approach, fluid flow, stress-strain, ingot mould filling

Abstract

One of the critical challenges encountered when modeling a thermo-mechanical problem in the context of steel casting processes, is to achieve a concurrent and efficient computation of fluid flow (ingot mould filling, nozzle jet in continuous casting) and solid mechanics (stress-strain in solidified regions). This is of crucial importance in industry for the prediction of surface or sub-surface cracks for instance that may initiate in solidified regions during the filling stage of ingot casting, or in the mould region during continuous casting.

The current state-of-the-art [15-17-21] consists in separating the analysis in two distinct stages: fluid flow using CFD codes and stress-strain analysis using structural codes. This induces several drawbacks regarding practical use and computational efficiency. A monolithic formulation, treating the fluid-solid interaction (FSI) may be investigated but is not adapted to the context of solidification, because of huge differences between liquid viscosity and solid consistency. It is then preferable to consider this FSI problem as a weak interaction problem, for which a partitioned formulation is more efficient than a monolithic one. Therefore, a two-step resolution strategy combining fluid flow and solid mechanics has been developed. Liquid flow (natural convection or filling flow), thermal dilatation as well as thermally induced deformation of the solid phase are accounted for.

[1] Correspondence to : Okba Boughanmi
E-mail: okba.boughanmi@mines-paristech.fr

[2] E-mail : michel.bellet@mines-paristech.fr

1. INTRODUCTION

Ingot casting process is one of the most important processes in the steel-making industry. It involves filling of liquid metal in a mould and its solidification which should be treated simultaneously. For instance, during the filling of large steel ingots, up to 20% of the ingot volume may be already solidified at the end of mould filling, due to long filling times. Using CFD codes and Navier-Stokes modelling, it can be clearly understood that there is no chance to predict the occurrence of thermomechanical defects such as cracks in the solidified regions. On another hand, a structural thermomechanical simulation necessarily starts from a filled mould and, as a consequence, it fails to predict defects occurring during mould filling. In addition, this kind of approach fails in taking into account the low viscosities of liquid metal, and then generally underestimates liquid convection effects and the associated energy transport [11-14]. The situation is similar for continuous casting when it comes to predict cracks in the thin solidified shell formed in the mould region (primary cooling) where there is an intense fluid flow associated with the nozzle jet.

The major aim of the mould filling stage is to predict the location of the moving free surface and the advancement of solidification. There are mainly three numerical approaches used in the literature to update a free surface during a filling process: the Marker and Cell method, consisting in following imaginary particles [1], the VOF method, consisting on solving the transport equation for the fractional volume function [3-12] and the Level Set method, consisting on solving the transport equation for a signed distance to the interface separating the air to the injected material [6].

Furthermore, steel casting processes, during which the liquid metal changes of state due to solidification, provide a special type of fluid-structure interaction (FSI) problem. Numerical methods for the solution of the FSI problem can be classified as either monolithic or partitioned. In a monolithic approach, a single set of momentum and mass conservation equations, in the fluid and solid domains, is solved. Whereas, in a partitioned formulation, separated fluid and solid problems are solved and coupled. In his work, Heil et al [21], have defined an IFS parameter Q, as the ratio of the stress scales used in the non-dimensionalised forms of the solid and fluid equations, indicating the strength of the FSI. They concluded that, for a weak FSI problem (such as in the case of solidification problems), a partitioned approach is more efficient than a monolithic one. Furthermore, due to the large difference between liquid viscosity and solid consistency, most investigations using a monolithic formulation encounter serious problems, requiring additional assumptions specific to the study's purpose. In fact, in a liquid-type calculation analyzing fluid flow or macrosegregation, an assumption of a fixed and rigid solid can be considered [7]. However, in a solid-like calculation whose objective is studying the stress-strain evolution within the solidified metal, an augmented viscosity in the liquid metal should be taken to avoid systems conditioning problems [11-13-14].

In order to overcome such limitations and to achieve a concurrent calculation of fluid flow in liquid regions and stress-strain in solidified regions during solidification, a partitioned mechanical solution scheme is proposed in the present paper.

This partitioned mechanical approach is coupled to a temperature-based model for solve energy conservation with phase change. A "Level Set" method is applied for tracking the metal-air interface during ingot filling and further cooling. To improve solution quality and reduce computing time, a mesh adaptation technique based on a posteriori error estimator is used. To illustrate its capability, this new formulation is applied to the simulation of ingot mould filling coupled to solidification.

2. MODEL FORMULATION

2.1 Free Surface Modeling

A level set method [6] is applied for tracking the metal-air interface during the whole casting process: during mould filling, up to complete solidification. The level set function α is defined as the signed distance to the metal-air interface. By convention, $\alpha < 0$ corresponds to air, $\alpha > 0$ represents the metal, and $\alpha = 0$ defines the interface. Since the only useful information for our computation is the exact zero iso-value position, the standard distance function is truncated and approached by a sinusoidal filter, in order to limit advection calculations around the interface. The modified level set function $\phi(\alpha)$ writes [18-22]:

$$\phi(\alpha)=\begin{cases}\dfrac{2E}{\pi} & \alpha > E \\ \dfrac{2E}{\pi}\sin\left(\dfrac{\pi}{2E}\alpha\right) & -E < \alpha < E \\ -\dfrac{2E}{\pi} & \alpha < -E\end{cases} \quad (1)$$

where E is a thickness related to the local mesh size h_{mesh} ($E \in [10\ h_{mesh}, 20\ h_{mesh}]$).

The interface is then updated by time-integration of the convective reinitialization equation described below [18-22]:

$$\begin{cases}\dfrac{\partial \phi}{\partial t} + \left(\mathbf{v} + \lambda \mathbf{U}\right)\cdot \nabla \phi = \lambda s \\ \phi\left(t=0, \mathbf{x}\right) = \phi_0\left(\mathbf{x}\right)\end{cases} \quad (2)$$

where the parameters s, λ and **U** are defined as follows:

- $s(\phi)$ is the sign function verifying:
  $s(\phi) = -1$, if $\phi < 0$, $s(0) = 0$ and $s(\phi) = 1$, if $\phi > 0$
- λ is a parameter having the dimension of a velocity, and chosen to $h_{mesh}/\Delta t$, Δt denoting the time step;
- **U** is a unit vector defined by: $\mathbf{U} = s(\phi)\dfrac{\nabla \phi}{|\nabla \phi|}$.

The time derivative of the level set function is approached by an implicit Euler backward finite difference scheme. The convective reinitialization equation (2) is stabilised with a SUPG (Steamline-Upwind-Petrov-Galerking) method [4]. The standard test functions N are replaced by the SUPG test functions $\varphi = N + \tau_{SUPG}\tilde{\mathbf{v}}\cdot\nabla N$, where τ_{SUPG} is the SUPG stabilization parameter defined by:

$$\tau_{SUPG} = \frac{h_{mesh}}{D\|\tilde{\mathbf{v}}\|} \quad (3)$$

where:

- h_{mesh} is the mesh size along the flow direction defined by:

$$h_{mesh} = \frac{2\|\tilde{\mathbf{v}}\|}{\sum_{i=1}^{D}|\tilde{\mathbf{v}}\cdot\nabla N_i|} \quad (4)$$

- D is the number of nodes per element, equal to d + 1 (3 in 2D and 4 in 3D);
- $\tilde{\mathbf{v}}$ is the velocity vector estimated at the center of the element.

2.2 Mixed Material Properties

Using a monolithic approach for a thermomechanical problem, only one equation, for the metal and the air, must be solved for each conservation problem. Thus, all physical properties used in conservation equations should be mixed, in the elements close to the interface, as follows:

$$[\Psi] = F(\phi)\Psi_m + (1 - F(\phi))\Psi_a \quad (5)$$

where Ψ_m and Ψ_a are respectively the corresponding properties of the metal and the air (Fig. 1) and $F(\phi)$ is a "smoothed Heaviside function" [8], illustrating the metal presence in the cavity, defined by:

$$F(\phi) = \begin{cases} 1 & \phi > e \\ \frac{1}{2}\left(1 + \frac{\phi}{e} + \frac{1}{\pi}\sin(\frac{\pi}{e}\phi)\right) & -e < \phi < e \\ 0 & \phi < -e \end{cases} \quad (6)$$

where e is the thickness of the mixture related to the local mesh size h_{mesh} ($e \in [\, h_{mesh}, 2\, h_{mesh}]$).

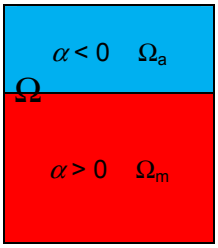

Figure 1: Air-metal mixture

2.3 Two-Step Coupled Formulation for the Mechanical Modeling

The main limitation of a monolithic formulation is to take into account a low viscous liquid and an elastic visco-plastic solid. To overcome this limitation, a 2-step resolution strategy have been developed, which consists in dividing the mechanical problem into two coupled sub-problems (Fig. 2):

- a solid-type formulation from which we can calculate the velocity, stresses and distortions using arbitrary augmented viscosities in the liquid metal and in the air ;
- a liquid-type formulation which permits to model fluid flow and compute the velocity and pressure fields in the liquid phase and in the air.

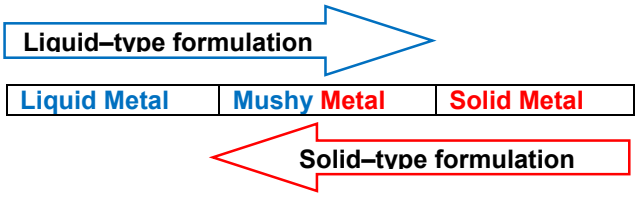

Figure 2: Two-step approach coupling fluid and solid mechanics

2.3.1 First Step: Solid-Type Formulation

Constitutive Equations

In the first step, the approach proposed by Bellet et al. [11-14] is applied. A thermo-viscoplastic (TVP) model is used to model the behavior of the metal in the liquid and mushy state. A small strain thermoelastic-viscoplastic (TEVP) model is used for the solid state. The different behaviors of the metal are distinguished by a critical transition temperature T_c chosen equal to the solidus temperature in the present work.

For the TVP behavior, we use a non-linear Norton-Hoff law, including a term for thermal dilatation representing the solidification shrinkage within the mushy metal:

$$\dot{\boldsymbol{\varepsilon}} = \dot{\boldsymbol{\varepsilon}}^{vp} + \dot{\boldsymbol{\varepsilon}}^{th} \quad (7)$$

$$\dot{\boldsymbol{\varepsilon}}^{vp} = \frac{1}{2K_{vp}}\left(\sqrt{3}\dot{\bar{\varepsilon}}\right)^{1-m_{vp}(T)}\mathbf{s} \quad (8)$$

$$\dot{\boldsymbol{\varepsilon}}^{th} = -\frac{\rho_s - \rho_l}{3\rho_l}\frac{\partial g_s}{\partial t}\mathbf{I} \quad (9)$$

$\dot{\boldsymbol{\varepsilon}}^{vp}$ and $\dot{\boldsymbol{\varepsilon}}^{th}$ are respectively, the viscoplastic and the thermal strain rate tensors, $\mathbf{s}$ the stress deviator tensor, K_{vp} is the viscoplastic consistency, m_{vp} the strain rate viscoplastic sensitivity, $\dot{\bar{\varepsilon}}$ is the Von-Mises equivalent strain rate and $\mathbf{I}$ is the identity tensor.
The well known power law relating stress and inelastic strain rate von Mises invariants; can be obtained from equation (8):

$$\bar{\sigma} = K_{vp}\left(\sqrt{3}\right)^{m_{vp}+1}\dot{\bar{\varepsilon}}^{m_{vp}} \quad (10)$$

In the solidification interval, rheological viscoplastic parameters K_{vp} and m_{vp} depend on the solid fraction according to empirical models.

For the TEVP behavior, we use a multiplicative type threshold law. In this case, the thermal dilatation term represents the linear thermal expansion within the solid metal:

$$\dot{\boldsymbol{\varepsilon}} = \dot{\boldsymbol{\varepsilon}}^{el} + \dot{\boldsymbol{\varepsilon}}^{vp} + \dot{\boldsymbol{\varepsilon}}^{th} \tag{11}$$

$$\dot{\boldsymbol{\varepsilon}}^{el} = \frac{1+\nu}{E}\dot{\boldsymbol{\sigma}} - \frac{\nu}{E} tr(\dot{\boldsymbol{\sigma}})\mathbf{I} \tag{12}$$

$$\dot{\boldsymbol{\varepsilon}}^{vp} = \frac{\sqrt{3}}{2\overline{\sigma}} \left\langle \frac{\overline{\sigma} - \sigma_y}{\sqrt{3}K_{evp}} \right\rangle^{1/m_{evp}(T)} \mathbf{s} \tag{13}$$

$$\dot{\boldsymbol{\varepsilon}}^{th} = -\frac{1}{3\rho_m}\frac{\mathrm{d}\rho_m}{\mathrm{d}t}\mathbf{I} \tag{14}$$

Equation (12) is a simplified form of the hypoelastic Hooke's law, where E is the Young's modulus, ν the Poisson's coefficient. $\dot{\boldsymbol{\sigma}}$ is a time derivative of the stress tensor $\boldsymbol{\sigma}$. Equation (13) gives the relation between the viscoplastic strain rate $\dot{\boldsymbol{\varepsilon}}^{vp}$ and the stress deviator $\mathbf{s}$ in which σ_y denotes the initial yield stress.
The scalar equation relating stress and viscoplastic von Mises invariants is given by:

$$\overline{\sigma} = \sigma_y + K_{evp}\left(\sqrt{3}\right)^{m_{evp}+1}\dot{\bar{\varepsilon}}^{m_{evp}} \tag{15}$$

Interaction with Liquid

The calculation encompasses the liquid region, but with a Newtonian behaviour which is a particular case of the non-Newtonian one, taking m_{vp}=1 and $K_{vp}=\eta_{l,1}$ in equations (7-9). Where, $\eta_{l,1}$ is an arbitrary high dynamic viscosity in order to generate a hydrostatic stress state.

Conservation Equations

In the solid-type formulation, the momentum and the mass conservation equations are, respectively, governed by the following equations:

$$\nabla\cdot\boldsymbol{\sigma} + [\rho]\mathbf{g} - [\rho]\boldsymbol{\gamma} = \nabla\cdot\mathbf{s} - \nabla p + [\rho]\mathbf{g} - [\rho]\frac{d\mathbf{v}}{dt} = 0 \tag{16}$$

$$\nabla\cdot\mathbf{v} - tr(\dot{\boldsymbol{\varepsilon}}^{th} + \dot{\boldsymbol{\varepsilon}}^{el}) = 0 \tag{17}$$

where $\boldsymbol{\sigma}$ is the stress tensor, $\mathbf{g}$, the gravity vector and p the pressure.
The weak form of equations (16-17) is discretized using the P1+/P1 element. The velocity field is linear continuous including additional degrees of freedom at the centre of the element (bubble formulation), and the pressure is linear continuous [11-14].

We note ($\mathbf{v_1}$, p_1) the velocity and pressure fields deduced from the 1st step calculation.

2.3.2 Second step: Liquid-Type Formulation

Constitutive Equations

The behavior of the liquid in this second step is chosen to be Newtonian quasi-incompressible using the effective dynamic viscosity in the liquid state ($\eta_{l,2} \sim 10^{-3}$ Pa.s) and an augmented temperature-dependent viscosity is the mushy state (Eq. (19)). The fluid flow is caused by the density difference between the solid and the liquid phases (shrinkage-induced flow) and by the thermal gradients in presence of gravity (natural convection).

$$\dot{\boldsymbol{\varepsilon}} = \dot{\boldsymbol{\varepsilon}}^{vp} + \dot{\boldsymbol{\varepsilon}}^{th} \tag{18}$$

$$\dot{\boldsymbol{\varepsilon}}^{vp} = \frac{1}{2\eta_{l,2}}\mathbf{s} \tag{19}$$

$$\dot{\boldsymbol{\varepsilon}}^{th} = -\frac{\rho_s - \rho_l}{3\rho_l}\frac{\partial g_s}{\partial t}\mathbf{I} \tag{20}$$

Interaction with solid

For nodes belonging to solid elements, the velocity of liquid is prescribed equal to solid velocity (known from first step): $\mathbf{v}_2^{imp} = \mathbf{v}_1$

Conservation Equations

In the liquid-type formulation, the momentum and mass conservation equations are respectively:

$$\nabla\cdot\boldsymbol{\sigma} + [\tilde{\rho}]\mathbf{g} - [\tilde{\rho}]\boldsymbol{\gamma} = \nabla\cdot\mathbf{s} - \nabla p + [\tilde{\rho}]\mathbf{g} - [\tilde{\rho}]\frac{d\mathbf{v}}{dt} = 0 \tag{21}$$

$$\nabla\cdot\mathbf{v} - tr(\dot{\boldsymbol{\varepsilon}}^{th}) = 0 \tag{22}$$

$[\tilde{\rho}]$ is the air-metal mixed buoyancy term according to the Boussinesq approximation:

$$[\tilde{\rho}] = F(\phi)\tilde{\rho}_m + (1 - F(\phi))\tilde{\rho}_a$$

where:

$$\tilde{\rho}_m = \rho_{m_0}\left(1 - \beta_{T_m}(T - T_0)\right)$$
$$\tilde{\rho}_a = \rho_{a_0}\left(1 - \beta_{T_a}(T - T_0)\right)$$

β_{T_m} and β_{T_a} are respectively the thermal expansion coefficients of metal and air.
The stabilization of Navier-Stokes equations is achieved using SUPG-PSPG (Pressure Stabilizing Petrov/Galerkin) formulation [9].
We note $(\mathbf{v}_2, p_2)$ the velocity and pressure fields deduced from the 2nd step calculation.

2.4 Thermal Modeling

Solidification processes involve heat transfer with liquid-solid phase change. The energy conservation equation is solved by a time-dependent conduction-convection equation:

$$\left[\rho c_{p_{eff}}\right]\left(\frac{\partial T}{\partial t} + \mathbf{v}_2\cdot\nabla T\right) - \nabla\cdot([k]\nabla T) = 0 \tag{23}$$

Parameters $\rho, c_{p_{eff}}, k$ and $\mathbf{v}_2$ denote respectively the density, the effective specific heat, the heat conductivity and the velocity vector resulted from the liquid-type calculation.

Mixed parameters $\lfloor \rho c_{p_{eff}} \rfloor$ and $[k]$ are given by the following expressions:

$$\lfloor \rho c_{p_{eff}} \rfloor = \rho c_{p_{eff_m}} F(\alpha) + \rho c_{p_a} (1 - F(\alpha))$$
$$[k] = k_m F(\alpha) + k_a (1 - F(\alpha))$$

Equation (23) is solved for the temperature *T* and completed with an enthalpy-based approach. The phase-change during metal solidification is treated using the approach proposed by Morgan [2]. The effective specific heat in the metal is approximated by the following regularization formula:

$$c_{p_{eff_m}} = \frac{H^t - H^{t-\Delta t}}{T^t - T^{t-\Delta t}} \quad (24)$$

where, the specific enthalpy of the metal is defined by:

$$H = \int_{T_{ref}}^{T} c_{p_m} d\tau + f_l L \quad (25)$$

Here c_{p_m}, f_l and L denote respectively the metal specific heat, the liquid mass fraction and the latent heat of fusion. The liquid fraction is defined a priori as a function of temperature.
The diffusive part of equation (23) is stabilized using the Residual Free Bubble (RFB) method [16] while the convective part is stabilized by the shock capturing Petrov-Galerkin (SCPG) method [5].

2.5 Mesh Adaptation Technique

In order to reduce computing time and to reach the numerical solution with a desired accuracy, an anisotropic mesh adaptation technique is used. Mesh adaptation is guided by *a posteriori* directional error estimator.

2.5.1 The a Posteriori Error Estimator

Following [10], it is assumed here that the interpolation error can serve as a good indicator for mesh adaptivity. Considering a P1 finite element discretization of a scalar field *u*, this interpolation error can be upper-bounded in each element *K* by the formula:

$$\|e\|_{\infty,K} \le c \max_{x \in K} \max_{a \in K} \left(\mathbf{a} \cdot |\mathbf{H}_u(\mathbf{x})| \mathbf{a} \right) \quad (26)$$

where $\mathbf{H}_u$ is the Hessian matrix of *u* (matrix of second spatial derivatives), **a** denotes the 6 edge vectors of the element and *c* is a constant. $\mathbf{H}_u$ can be decomposed as $\mathbf{H}_u = \mathbf{R} \Lambda \mathbf{R}^T$ where **R** is the eigenvectors matrix and $\Lambda = diag(\lambda_k)$ the diagonal matrix of eigenvalues. Relation (26) means that denoting h_K the dimension of the element along one of the eigen directions of $\mathbf{H}_u$, of eigen value λ_k, the error in this direction varies like $h_k^2 \lambda_k$.

2.5.2 Metric Construction

A mesh metric tensor based on a discrete approximation of the solution Hessian is constructed [19]. It takes the form: $\mathbf{M} = \mathbf{R} \tilde{\Lambda} \mathbf{R}^T$, where $\tilde{\Lambda} = diag(\tilde{\lambda}_k)$, $\tilde{\lambda}_k$ are the modified eigenvalues of the Hessian matrix. To obtain a suitable mesh resolution, the interpolation error should be uniformly distributed within each direction which leads to: $c h_k^2 \tilde{\lambda}_k = \varepsilon$. ε is the user specified tolerance for the error and h_k is the desired size in the kth principal direction. To limit the mesh size and avoid singular metrics, two truncation values h_{min} and h_{max} are introduced in the metric definition. Finally, the modified eigenvalues of the Hessian matrix become:

$$\tilde{\lambda}_i = \min\left(\max\left(\frac{c\lambda_i}{\varepsilon}, \frac{1}{h_{\max}^2} \right), \frac{1}{h_{\min}^2} \right) \quad (27)$$

2.6 Time-step control

The resolution of the coupled mechanical problem is desynchronized. Actually, we distinguish two time-steps for each sub-problem: Δt_1 for step 1 and Δt_2 for step 2, which verify: $\Delta t_1 = n \Delta t_2$ (n=10 in this work). The time step Δt_2 is computed according to the mesh size along the flow direction defined in Eq. (4):

$$\Delta t_2 \le \frac{h_{mesh}}{2\|\tilde{\mathbf{v}}\|} \Rightarrow \Delta t_2 = \min_K \left(\frac{h_{mesh}^K}{2\|\tilde{\mathbf{v}}\|} \right) = \min_K \left(\frac{1}{\sum_{i=1}^{D} |\tilde{\mathbf{v}} \cdot \nabla N_i|} \right) \quad (28)$$

2.7 Resolution Strategy

At each time increment, the resolution algorithm is divided in 8 modules:

1- execution of conditional filling model;
2- energy equation resolution, providing temperature and liquid fraction;
3- step 1 calculation to obtain the velocity, stresses and distortions in the solidified regions;
4- step 2 calculation to obtain velocity in the liquid regions as well as air velocity and pressure;
5- resolution of the modified transport equation to update the air-metal level set;
6- mixture of thermo-physical properties;
7- application of the mesh adaptation technique when necessary;
8- time-step control

3 APPLICATION TO MOULD FILLING AND COOLING

Problem description

The physical system for the present study consists of a three-dimensional parallelepipedic mould of height 50 mm, width 40 mm and thickness 2.5 mm. A schematic representation of the physical system is shown in Fig. 3. Liquid steel enters through the bottom inlet Ω_0 with a temperature of 1550°C and a velocity of 0.1m.s^{-1}. A riser of dimension 10 mm x 10 mm x 2.5 mm is provided at the top of the mould in order to eject the air (initially at T=800°C) as filling of liquid steel progresses. In order to study a planar problem, two symmetry surfaces located in z=0 and z =2.5mm are considered. The materials properties are summarized in Table 1. The mechanical and thermal boundary conditions (B.C) which vary during filling and cooling are prescribed in tables 2 and 3. Figure 4 shows surfaces where heat extraction occurs during filling and cooling stages. These surfaces are defined as the intersection of the boundary walls of the cavity and a second metal presence function defined by the following Heaviside function $A(\phi)$:

$$A(\phi) = \begin{cases} 1 & \phi > e \\ 0 & \phi \le e \end{cases} \qquad (29)$$

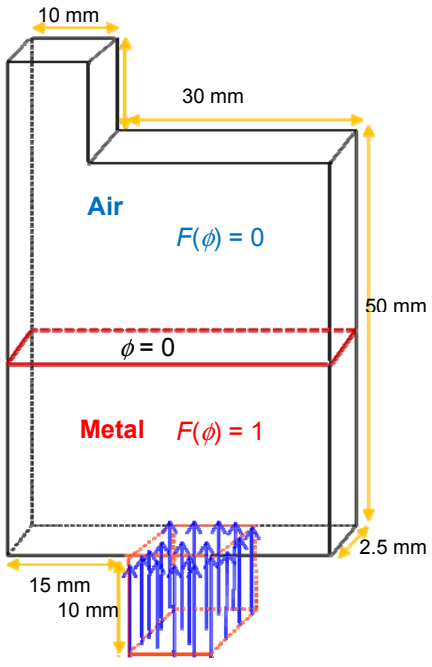

Figure 3: Ingot geometry

Metal properties			
$g_l(T)$	$g_l(T) = (T - T_S)/(T_L - T_S)$	T_{m_0}	1550°C
$c_{p_m}(T)$	$c_{p_m}(T) = c_{p_l} g_l + c_{p_s} g_s$ $c_{p_l} = 717, c_{p_s} = 688 \left(\text{J.kg}^{-1}.\text{K}^{-1}\right)$	h	10^3 W.m^{-2}.K^{-1}
		T_{ext}	200°C
$k_m(T)$	$k_m(T) = k_l g_l + k_s g_s$ $k_l = 34, k_s = 32 \left(\text{W.m}^{-1}.\text{K}^{-1}\right)$	L	260000 J.kg^{-1}
		T_S	1425°C
$\eta_{m_2}(T)$	$\log\left(\eta_{m_2}(T)\right) = aT + b; T \in [T_l, T_s]$ $\eta_{l_2} = 10^{-3}, \eta_{s_2} = 10^5 \left(\text{Pa.s}\right)$	T_L	1478°C
		T_{Fill}	1550°C
ρ_l	7060 kg.m^{-3}	v_{Fill}	0.1 m.s^{-1}
ρ_s	7303 kg.m^{-3}	β_{T_m}	7.2 10^{-5} K^{-1}
TVP : $K_{vp}(T)$, $m_{vp}(T)$, $\eta_{l_1} = 10$ Pa.s			
TEVP : $K_{evp}(T)$, $m_{evp}(T)$, $E(T)$, $\sigma_y(T)$, ν=0.33			

Air properties			
c_{p_a}	1006 J.kg^{-1}.K^{-1}	T_{a_0}	800°C
k_a	0.0242 W.m^{-1}.K^{-1}	β_{T_a}	3.85 10^{-4} K^{-1}
η_{a_1}	1 Pa.s	η_{a_2}	10^{-4} Pa.s
ρ_a	1.125 kg.m^{-3}		

Table 1: Thermophysical properties used in the simulation

Surface	Mech B.C	Thermal B.C
z = 0, z = 2.5 mm	**v**$_1$. **n** = 0 **v**$_2$. **n** = 0	-[k]∇T. **n** = 0
$\partial(\Omega - \Omega_0) * A(\phi)$	**v**$_1$. **n** = 0 **v**$_2$. **n** = 0	$-k_m \nabla T$. **n** = $h(T - T_{ext})$
$\partial(\Omega - \Omega_0) * (1 - A(\phi))$	**v**$_1$. **n** = 0 **v**$_2$. **n** = 0	$-k_a \nabla T$. **n** = 0
$\partial\Omega_0$	**v**$_1$. **n** = 0	
Volume		
Ω_0	**v**$_2$= **v**$_{Fill}$	$T = T_{Fill}$

Table 2: Boundary conditions during filling stage

Surface	Mech B.C	Thermal B.C
z = 0 **z = 2.5 mm**	**v**$_1$. **n** = 0 **v**$_2$. **n** = 0	-[k]∇T . **n** = 0
$\partial\Omega * A(\phi)$	**v**$_1$. **n** = 0 **v**$_2$. **n** = 0	$-k_m \nabla T$. **n** = $h(T - T_{ext})$
$\partial\Omega * (1 - A(\phi))$	**v**$_1$. **n** = 0 **v**$_2$. **n** = 0	$-k_a \nabla T$. **n** = 0

Table 3: Boundary conditions during cooling stage

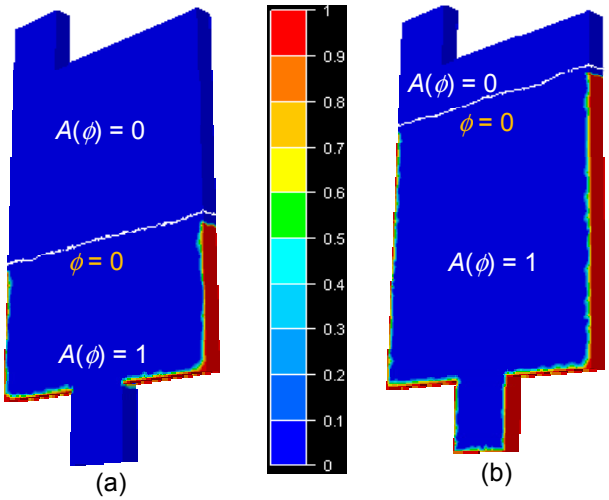

Figure 4: Surfaces where heat extraction occurs:
(a) during filling stage (b) during cooling stage

Mould filling process

We have chosen to get the user the possibility to fix the volume of the filled metal in the cavity. Therefore, a filling ratio given by the proportion of metal volume to the total volume of the cavity should be introduced. It distinguishes between the filling and the cooling stages and is chosen equal to 0.8 in this simulation.

Figure 5 illustrates the filling sequence where the zero-isovalue of the level set function representing the metal/air interface is shown at various times. Initially the liquid steel flows towards the right and left walls and impinges on them as seen in Fig.5 (t=0.134 s). This causes an interaction between the returning flow and the incoming flow from the bottom inlet. This interaction leads to the air trapping observed at t = 0.21 s. As filling proceeds, the waviness of the interface reduces and at approximately 0.6 s, the interface becomes almost flat, indicating a smooth mould filling subsequently. The filling criterion is reached at approximately t_{Fill} = 1.718 s.

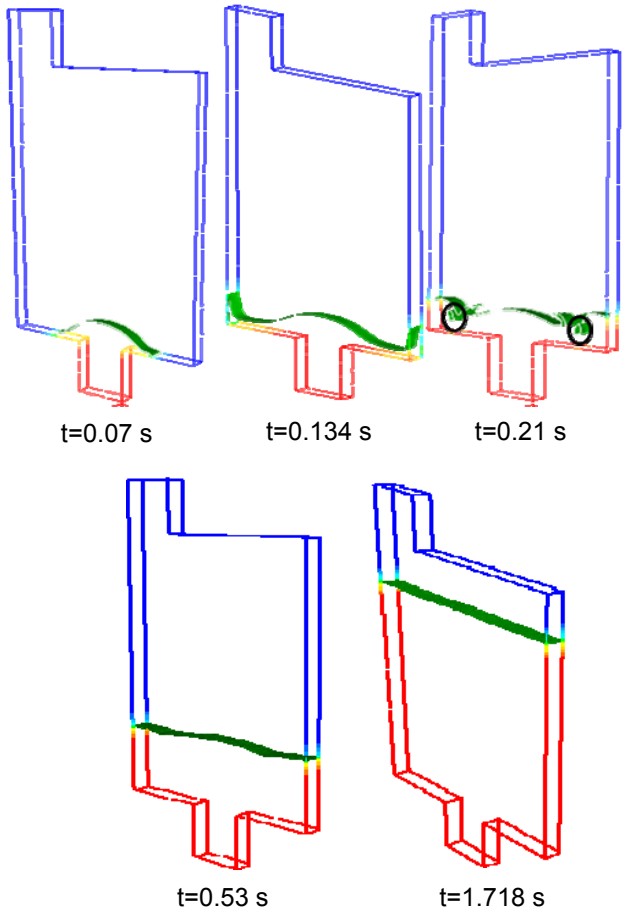

Figure 5: Mould filling sequence, using interface capturing by a level set function

Adaptive remeshing technique

Simulations are performed using the adaptive remeshing technique based on the combination of the error distribution of two objective functions (Fig.6):

- the "smoothed Heaviside function" $F(\phi)$ illustrating the metal presence in the cavity defined by Eq. 6;
- a function resulting from the liquid-type calculation and defined as the ratio between the norm velocity vector $\|\mathbf{v}_2\|$ and its maximum value v_{2max}.

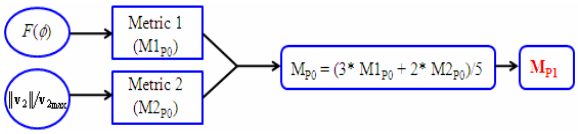

Figure 6: Metrics combination principle

Figure 7 shows the distribution of mesh size illustrating mesh refinement at interfaces, as well as in convection loops formed after the end of filling.

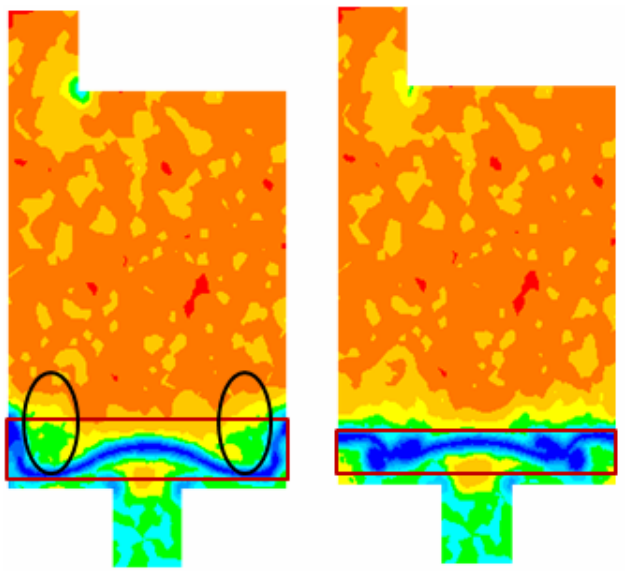

t = 0.155 s
h_{min} = 0.25 mm h_{max} =1.7 mm

t = 0.215 s
h_{min} = 0.24 mm h_{max} =1.7 mm

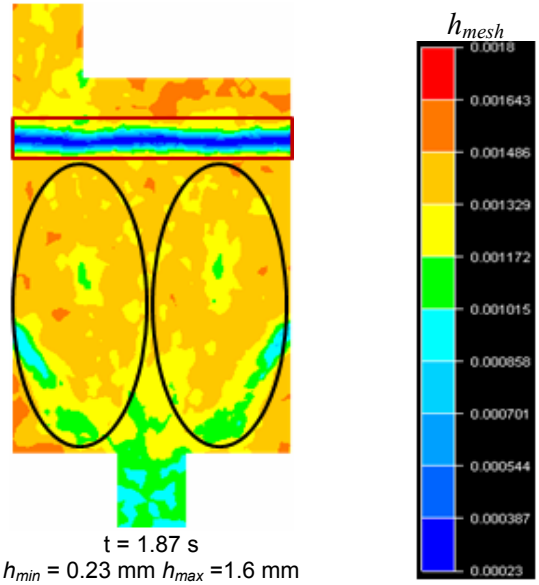

t = 1.87 s
h_{min} = 0.23 mm h_{max} =1.6 mm

Figure 7: Mesh size distribution

Fluid Flow versus Strain-Stress in the Solid Metal

Figures 8 and 9 show the flow field illustrated in terms of the velocity vectors and the distribution of the σ_{yy} stress in the solidified regions during the filling stage (t = 0.85 s and t = 1.52 s) and the cooling stage (t = 2.14 s and t = 3.1 s). The maximal value of the liquid velocity is reached at about 0.72 s ($V_{liq,\ max}$ = 24.5 cm.s^{-1}). We note that, cooled metal descends along the solid-liquid interface while hotter metal ascends in the middle of the cavity.

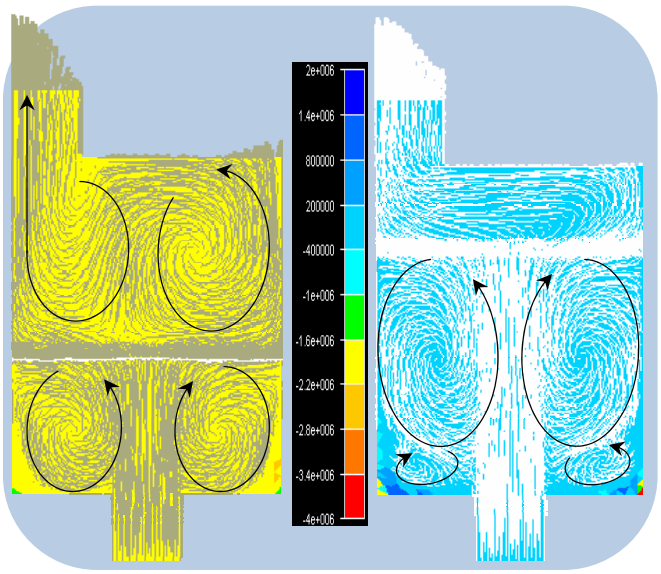

(a)
t = 0.85 s
$v_{Liq,\ max}$ = 20 cm/s
$\sigma_{yy,\ max}$= 0.48 MPa
$\sigma_{yy,\ min}$ = -0.9 MPa

(b)
t = 1.52 s
$v_{Liq,\ max}$ = 16.4 cm/s
$\sigma_{yy,\ max}$= 1.6 MPa
$\sigma_{yy,\ min}$ = -3.47 MPa

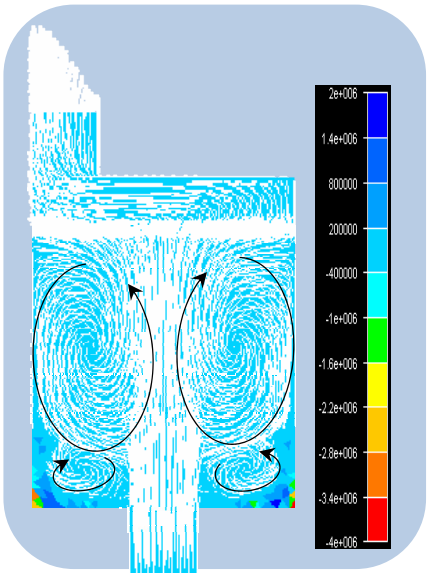

(c)
t = 1.718 s (end of the filling stage)
$v_{Liq,\ max}$ = 18 cm/s
$\sigma_{yy,\ max}$= 1.77 MPa
$\sigma_{yy,\ min}$ = -4.23 MPa

Figure 8: Fluid flow and vertical stress in the solid steel during filling stage in section z = 0

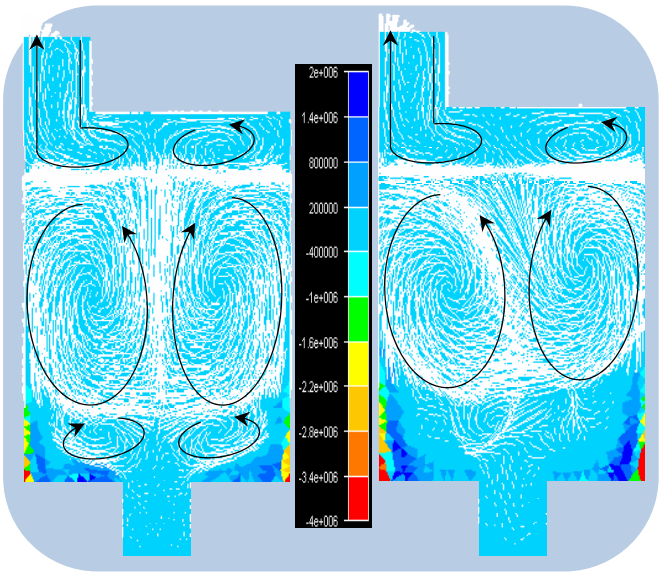

(a)
t = 2.14 s
$v_{Liq,\ max}$ = 14.8 cm/s
$\sigma_{yy,\ max}$= 1.9 MPa
$\sigma_{yy,\ min}$ = -4.56 MPa

(b)
t = 3.1 s
$v_{Liq,\ max}$ = 12.6cm/s
$\sigma_{yy,\ max}$= 2.5 MPa
$\sigma_{yy,\ min}$ = -6.34 MPa

Figure 9: Fluid flow and vertical stress in the solid steel during cooling stage in section z = 0

Two symmetric thermally induced convection loops due to the temperature gradient fill most of the cavity. We observe also two secondary circulation loops in the metal representing the residual flow which opposes the buoyancy induced flow. The residual flow is generated since the filling stage and diminishes during the cooling stage. (Figs. 8b, 9a and 9b).

The temperature evolution along the horizontal profile (y = 2.5 mm, z = 0) at the same times is shown in Fig.10. We note that the solidification front advances faster in the bottom part of the cavity (Fig.11).

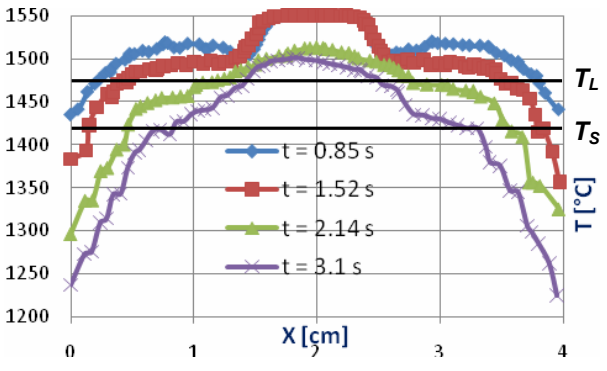

Figure 10: Temperature evolution along the horizontal profile (y = 2.5 mm, z = 0) at different times

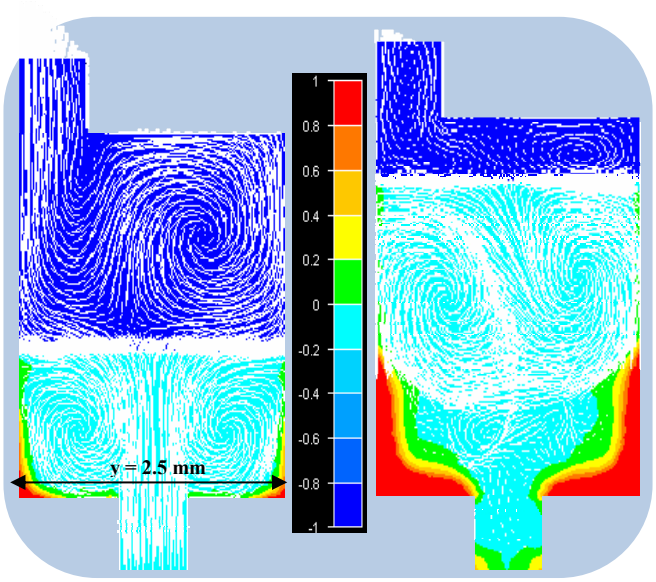

(a)
Filling stage, t = 0.85 s

(b)
Cooling stage, t = 3.1 s

Figure 11: Fluid flow and solid fraction (g_s) in section z = 0. By convention, g_s=-1 in the air (dark blue zone).

Mass conservation

Since the free surface evolves during filling and cooling stages, the steel mass conservation should be checked. An error parameter representing the relative difference between numerical and theoretical mass is given by the following expressions:

During filling stage:

$$Err(t) = \frac{m_{num}(t) - m_{theo}(t)}{m_{theo}(t)} \quad \text{for } t \le t_{Fill} \tag{30}$$

During cooling stage:

$$Err(t) = \frac{m_{num}(t) - m_{theo}(t_{Fill})}{m_{theo}(t_{Fill})} \quad \text{for } t > t_{Fill} \tag{31}$$

where:

- t_{Fill} denotes the time at which of filling stage ends
- m_{num} denotes the computed steel mass defined by:

$$m_{num}(t) = \int_{\Omega} F(\phi)(t)\rho_m(t)dV$$

- m_{theo} denotes the theoretical steel mass defined by:

$$m_{theo}(t) = m_0 + \rho_{m,T=T_{Fill}} \, v_{Fill} S_{Fill} t$$

$$m_0 = |\Omega_0| \rho_{m,T=T_{Fill}}$$

m_0 being the steel mass at the inlet volume Ω_0, ρ_m the steel density and S_{Fill} is the filling surface.

We have verified that the steel mass is conserved and the little overshoot of the mass is due to the air-metal mixture around the interface (Fig.12).

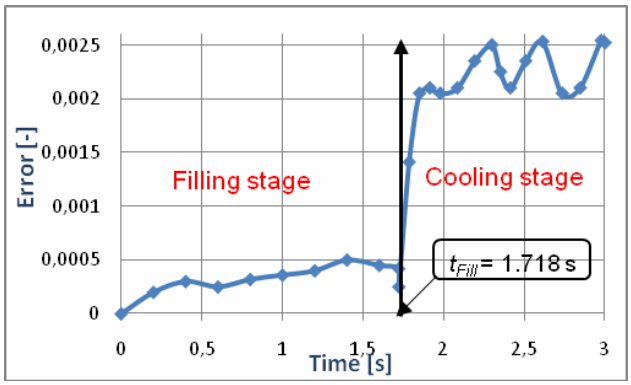

Figure 12: Mass error evolution during filling and cooling stages

CONCLUSION AND FUTURE RESARCH

A full simulation of a filling-cooling process has been studied in this work. A 2-step finite element formulation coupling fluid and solid mechanics has been developed. The limitation of an augmented liquid viscosity has been resolved. A concurrent computation of fluid flow and solid mechanics has been achieved. Future work will consist on the application of this approach to the simulation of industrial ingot and continuous casting processes.

ACKNOWLEDGMENT

This work has been supported by the French National Research Agency “Agence Nationale de la Recherche” in the framework of the “Cracracks” project (07-MAPR-0008).

REFERENCES

[1] Welch, J.E.; Harlow, F.H.: The MAC method, a computing technique for solving incompressible, transient fluid flow problems involving free surface, Physics of Fluids 9 (1966) 842–851

[2] Morgan, K.; Lewis, R.W.; Zienkiewicz, O.C.: An improved algorithm for heat conduction problems with phase change, International Journal for Numerical methods in Engineering, 12 (1978), P. 223-235

[3] Hirt, C.W.; Nichols, B.D.: Volume of fluid (VOF) method for the dynamics of free boundaries, Journal of Computational Physics, 39 (1981), P. 201–225.

[4] Thomas; Hughes, T.J.R.: Recent progress in the development and understanding of SUPG methods with special reference to the compressible Euler and Navier-stokes equations. International Journal for Numerical Methods in Fluids, 7 (1987), P.1261–1275

[5] Galeao, A.; Carmo, E.G.D.: A consistent approximate upwind Petrov-Galerkin method for convection- dominated problems. Computer Methods in Applied Mechanics and Engineering, 68(1) (1988), P: 83–95

[6] Osher, S.; Sethian, J.: Fronts propagating with curvature-dependent speed: algorithms based on Hamilton-Jacobi formulations, Journal of Computational Physics, 79 (1988), P. 12-69

[7] Chiang, K.C.; Tsai, H.L.: Interaction between shrinkage-induced fluid flow and natural convection during alloy solidification, International Journal for Heat and Mass Transfer, 35 (1992), P. 1771-1778

[8] Sussman, M.; Almgren, A.; Bell, J.; Colella, P.; Howell, L.; Welcomey, M.: An Adaptive Level Set Approach for Incompressible Two-Phase Flows, Journal of Computational Physics, 148-81 (1999)

[9] Tezduyar, T.E.; Osawa, Y.: Finite element stabilization parameters computed from element matrices and vectors, Comput. Methods Appl. Mech. Engrg., 190 (2000), P: 411-430

[10] Alauzet, F. ; Frey, P.J. ; Estimateur d'erreur géométrique et métriques anisotropes pour l'adaptation de maillage : Partie 1 : aspects théoriques. Technical report, INRIA, Rocquencourt, (2003)

[11] Bellet, M.; Fachinotti, V.D.: ALE method for solidification modeling, Computer Methods in Applied Mechanics and Engineering, 193 (2004), P: 4355-4381

[12] Bellet, M.; Saez, E.; Jaouen, O.; Coupez, T.: A 3D-FEM solver for non steady state Navier-Stokes equations with free surface. Application to mold filling simulation in casting processes, Symposium on Multiphase Phenomena and CFD Modelling and Simulation in Materials Processes, TMS Annual Meeting, Charlotte (NC, USA) March 2004, Proc. ed. by L. Nastac and B.Q. Li, The Minerals, Metals & Materials Society, (2004), P. 209-218

[13] Cruchaga, M.A.; Celentano, D.J.; Lewis, R.W.: Modelling fluid-solid thermo-mechanical interactions in casting processes, International journal for Numerical Methods in Heat & Fluid Flow, 14-2 (2004), P.167-186

[14] Bellet, M.; Jaouen, O.; Poitrault, I.: An ALE-FEM approach to the thermomechanics of solidification processes with application to the prediction of pipe shrinkage, International Journal for Numerical Methods in Heat & Fluid Flow, 15-2 (2005), P: 120-142

[15] Felippa, C.A.: Underwater shock on stipend shells: the source of Staggered Solution Procedure. 5th international Conference on Computational of Shell & Spatial Structures. IASS-IACM, (2005)

[16] Russo, A.; Brezzi, F.; Marini, L.D.: On the choice of a Stabilizing Subgrid for Convection Diffusion Problems. Comput. Methods Appl. Mech. Engrg., 194(2-5), (2005), P: 127-148

[17] Brenk, M.; Bungartz, M.: Fluid-structure interaction on cartesian grids: flow simulation and coupling environment, Fluid–structure interaction. LNCSE, 53. Springer, Heidelberg, (2006), P: 233–269

[18] Coupez, T. : Réinitialisation convective et locale des fonctions Level Set pour le mouvement de surfaces et interfaces, Journées Activités Universitaires de Mécanique, La Rochelle, France (2006)

[19] Hamide, M.; Massoni, E.; Bellet, M.: Adaptative mesh technique for thermal-metallurgical simulation of arc welding processes, International Journal for Numerical Methods in Engineering, 73 (2008), P. 624-641

[20] Heil, M.; Hazel, A.L.; Boyle, J.: Solvers for large-displacement fluid-structure interaction problems: segregated versus monolithic approaches, Computational Mechanics, 43 (2008), P: 91-101

[21] Mehl, M.; Brenk, M.: An Eulerian approach for partitioned fluid–structure simulations on Cartesian grids, Computational Mechanics, 43 (2008), P: 91-101

[22] Ville, L.; Silva, L.; Coupez, T.: Convected Level Set method for the numerical simulation of Fluid Buckling, International Journal for Numerical Methods in Fluids, 1-6 (2008)